Effect of pressure on energy levels of Sm^{2+} in BaFCl and SrFCl

Y. R. Shen and W. B. Holzapfel
Fachbereich 6 (Physik), Universität-Gesamthochschule Paderborn, 33095 Paderborn, Germany
(Received 8 December 1994)

The fluorescence of Sm^{2+}:BaFCl and Sm^{2+}:SrFCl has been measured under pressures up to 8 GPa. The energy-level schemes of Sm^{2+} in the two host crystals are determined in this pressure range. The earlier problem in the crystal-field (CF) levels of the $^5D_2$ multiplet at ambient pressure due to an accidental degeneracy is solved from the pressure-induced line shifts of the fluorescence spectra. The pressure dependences of the CF parameters B_q^k are deduced from the variations of the CF splittings. According to the results for B_q^k, the intrinsic CF parameters $\overline{B}_k$ of the superposition model and their distance dependences (power-law exponents) t_k ($k = 4$ and 6) are derived for Cl^- and for F^-. In comparison with other systems of trivalent and divalent lanthanide ions in host crystals with Cl^- or F^- ligands, it is concluded that (i) the intrinsic parameters $\overline{B}_4$ and $\overline{B}_6$ for both trivalent and divalent lanthanide ions with less than half-filled $4f$ shells are very similar to each other, and (ii) the power-law exponents t_k for divalent ions are larger than for trivalent ions. Furthermore, the intrinsic CF parameters $\overline{B}_k$ for F^- are systematically larger than those for Cl^-.

I. INTRODUCTION

Alkaline earth fluoride halides (MFX) doped with divalent lanthanide ions show a wide range of spectroscopic properties with many technological applications. Eu^{2+}:BaFBr is used in x-ray image plates and spectral hole burning has a potential use in optical data storage. In the search for high-temperature persistent hole burning, room temperature hole burning was realized in the inorganic mixed crystals Sm^{2+}:$SrFCl_{0.5}Br_{0.5}$.[1] Moreover, Sm^{2+}:SrFCl can be used as an improved luminescence pressure sensor.[2,3] This increasing number of potential applications has stimulated the present investigation on spectroscopic properties of divalent lanthanide ions under pressure.

Sm^{2+} in BaFCl and SrFCl was selected due to the excellent fluorescence features, which provide valuable information on the CF interactions between divalent lanthanide ions and both the Cl^- as well as the F^- ligand ions.

Divalent Sm^{2+} ions have a ground $4f^6$ configuration with the lowest spectral term ^7F and the first excited term ^5D, which split, respectively, into seven multiplets $^7F_0$ to $^7F_6$ and five $^5D_0$ to $^5D_4$ due to the spin-orbit interaction. With these splittings, the fluorescence spectra of Sm^{2+} are expected to resemble closely the isoelectronic situation of Eu^{3+}. However, the first excited $4f^55d^1$ configuration for Sm^{2+}, located in the visible and near UV region, is energetically much lower than for Eu^{3+}. This in turn affects various fluorescence features of the Sm^{2+}-doped crystals which are well known to depend on the relative position of the lowest $4f^55d^1$ levels with respect to the excited $^5D_0$ multiplet of $4f^6$. Therefore, the excitation mechanism of Sm^{2+} fluorescence is quite different than for trivalent lanthanide ions. The parity-allowed transition $4f^6 \rightarrow 4f^55d^1$ can generate notable fluorescence and offers enough intensity for the present fluorescence measurements under pressure.

II. EXPERIMENTAL DETAILS

The single crystals used for the present work were grown from high-purity compounds MF_2 and MCl_2 (99.99%) using the standard Bridgman-technique in the materials laboratory of the University of Paderborn. The samples contain a concentration of 0.1 mol. % Sm^{2+} ions.

The fluorescence of Sm^{2+}:BaFCl and Sm^{2+}:SrFCl was excited by two lines (488.0 nm and 514.5 nm) of an argon ion laser. The spectra were dispersed by a double grating spectrometer (Spex model 14018) and the fluorescence signal was detected by a Peltier cooled photomultiplier (model C31034) using standard photon counting. The entrance and output slit widths were typically set at 50–100 μm. The high-pressure and low-temperature fluorescence measurements were performed using a specially adapted diamond-anvil cell[4] (diameter 26 mm and height 20 mm), mounted on a closed cycle refrigerator (model 21SC cryodyne cryocooler).

A methanol-ethanol-water mixture (16:3:1) was used as a pressure transmitting medium. Pressure determinations at low temperature were made by the ruby fluorescence technique[5,6] as well as with the new luminescence pressure sensor Sm^{2+}:SrFCl[3].

III. STRUCTURAL ASPECTS

The fluoride chlorides ($MFCl$) crystallize in the tetragonal PbFCl-type structure (space group $P4/nmm$ or D_{4h}^7) with the metal cations in the $2c$ positions ($\frac{1}{4},\frac{1}{4},z_M$), the Cl anions in the $2c$ positions ($\frac{1}{4},\frac{1}{4},z_{Cl}$), and the F anions in the $2a$ positions ($\frac{3}{4},\frac{1}{4},0$) with respect to the origin at the symmetry center ($2/m$). The site symmetry of the cations is thereby $4mm(C_{4v})$. The cation coordination polyhedron is shown in Fig. 1. The cations are surrounded by nine anions, four equivalent F, four equivalent Cl anions, and one extra Cl anion marked as Cl′,

 ©1995 The American Physical Society

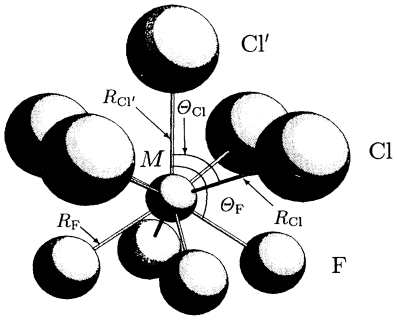

FIG. 1. Coordination polyhedron for the Cl^- and F^- ligands around the central ion M in $MFCl$.

which is located on the symmetry axis just above the M cation. R_F, R_{Cl}, and $R_{Cl'}$ denote the distances between the cation and the F, Cl, as well as Cl′ anions, respectively. Θ_F and Θ_{Cl} stand for the angles between the c-axis and the lines connecting the cation to F and Cl anions, respectively.

Other compounds belonging to the PbFCl-type structure are MFX, MHX, and MOX (X = Cl, Br, and I), thereby the PbFCl-type structure shows considerable variations with respect to the geometrical arrangements. The situation changes from a coordination lattice to a layered lattice when X varies from Cl to I. The variations in c/a ratios for this series at ambient pressure as well as its variation under pressure are successfully described within a simple hard-sphere model.[7]

For a complete structural determination, one needs the two lattice parameters a and c and the two atom position parameters z_M and z_X also under pressure. For BaFCl, z_M and z_X have been determined up to about 7 GPa (Ref. 8) and for PbFI up to about 5 GPa.[9] Thereby z_X stays constant within the experimental precision in both cases, but z_M increases by about 2.5% between 0 and 6 GPa for BaFCl and about 16% between 0 and 5 GPa for PbFI, which means that the metal cations move much more rapidly towards the X anion layer in PbFI than in BaFCl.

This movement is represented in Fig. 2, where the distance ratios $R_{X'}/R_X$ and the angles Θ_X are plotted versus the ionic radius ratios r_M/r_X for these compounds[10–14] at ambient pressure together with the corresponding results of PbFI and BaFCl under pressure. Thereby, the ionic radii for PbFCl and BaFCl under pressure are estimated from their linear compressibilities.[15] The different pressure behaviors of PbFI and BaFCl represent the typical characteristics of layered lattices on the one hand and coordination lattices on the other hand. With increasing pressure, corresponding to increasing r_M/r_X, a transition from layered lattices to coordination lattices is induced. These plots can then be used also to predict the stability limits of the PbFCl-type structure

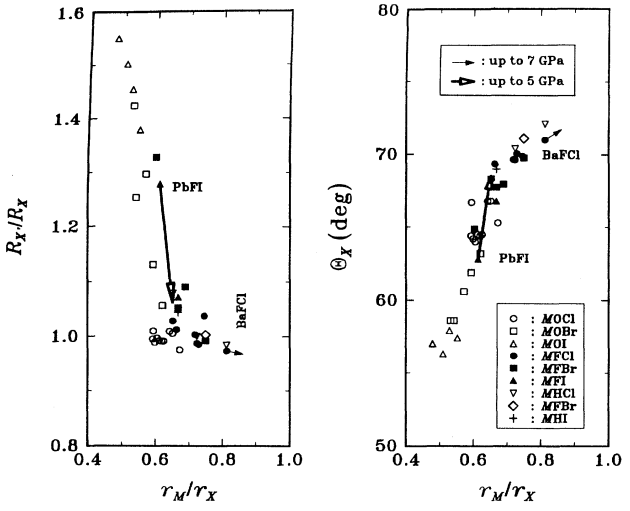

FIG. 2. $R_{X'}/R_X$ and Θ_X vs r_M/r_X for different MFX, MHX, and MOX compounds at ambient pressure and the effects of pressure in the cases of BaFCl and PbFI.

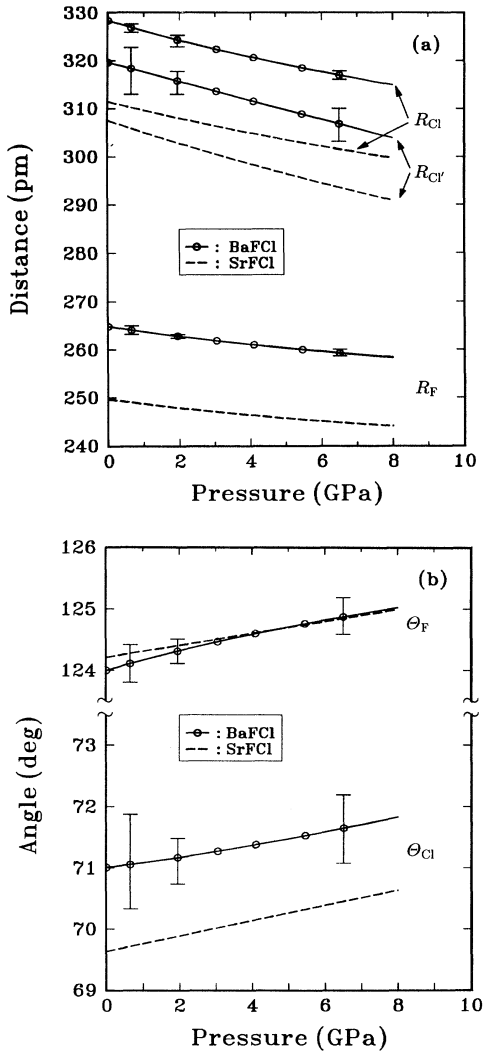

FIG. 3. (a) Variation of the distances R_{Cl}, $R_{Cl'}$, and R_F under pressure, (b) variation of the angles Θ_F and Θ_{Cl} under pressure.

under high pressure. A critical value of $r_M/r_X \approx 1$, where X anions are compressed to the size of M cations, seems to represent an upper limit for the stability of the PbFCl-type structure. This point has been verified by the observation on structural transitions for BaFCl at 21 GPa and for BaFBr at 27 GPa.[7]

According to the systematics in c/a under pressure[7] together with the results from Fig. 2, one can predict pressure dependences for the other compounds in the PbFCl-type structure. To obtain the structural parameters for SrFCl, one can assume that (i) the Cl position parameter for SrFCl is constant under pressure and equal to its ambient pressure value, $z_{Cl} = 0.643(1)$,[16] which is similar to the average value $z_X = 0.647(14)$ for all the other compounds with the PbFCl-type structure and corresponds also to the constant values z_X for BaFCl and PbFI under pressure, and (ii) the variation for the Sr position parameter under pressure is the same as for BaFCl, $dz_{Sr}/dp = dz_{Ba}/dp$, because both SrFCl and BaFCl belong to the region of coordination lattices. From these two assumptions and from the variation of the lattice parameters a and c under pressure,[7] the pressure dependences of the three distances and two angles are calculated, as shown in Fig. 3. In this figure, the results for BaFCl are recalculated using the new values of the lattice parameters a and c determined by Ref. 7 with much higher precison than previously.[8]

IV. SPECTRA AND ENERGY LEVELS OF Sm^{2+}

The absorption spectra of Sm^{2+}:BaFCl and Sm^{2+}:SrFCl were measured in an extended region to 50 000 cm^{-1} at 10 K and ambient pressure by the use of a standard spectrometer.[17] The corresponding transitions from the ground multiplet $^7F_0$ of the $4f^6$ to the $4f^55d^1$ configuration are illustrated in Fig. 4, which shows that (i) the absorption spectra of Sm^{2+} in BaFCl and SrFCl are very similar and (ii) the left-hand band edge for Sm^{2+}:SrFCl is about 1000 cm^{-1} lower than for Sm^{2+}:BaFCl, corresponding to the lower $4f^55d^1$ configuration of Sm^{2+}:SrFCl with respect to Sm^{2+}:BaFCl.

In early work,[18] the absorption spectrum of Sm^{2+}:BaFCl was measured only below $\approx$30 000 cm^{-1} and only the first four bands in Fig. 4 were observed. These four bands were explained in a simple model, in which the $4f^55d^1$ configuration is considered as a pure $5d^1$, corresponding to a much weaker interactions between the $5d$ and $4f$ electrons in comparison with CF effects on the $5d$ electrons. A $5d^1$ state in C_{4v} symmetry would split then into four CF levels corresponding to these four bands. This simple model, however, cannot describe the additional absorption bands above 30 000 cm^{-1} noticed in the present study. Earlier emission experiments[19] on Sm^{2+} in an ionized gas showed also characteristic multiplets of the $4f^55d^1$ configuration. Thus, one must take into account that the absorption spectra of Sm^{2+}:BaFCl and Sm^{2+}:SrFCl represent just this multiplet structure.

The fluorescence of Sm^{2+} in BaFCl and SrFCl was studied at 20 K up to 8 GPa. All the transitions from the crystal field levels of the multiplets $^5D_{0-2}$ to ^7F_J were

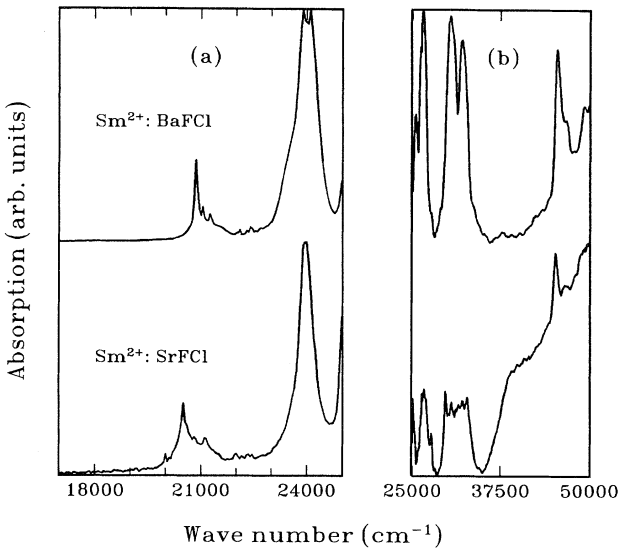

FIG. 4. Absorption spectra of Sm^{2+}:BaFCl and Sm^{2+}:SrFCl at 10 K and ambient pressure, using (a) halogen and (b) D_2 lamps as a light source.

observed except two transitions $^5D_0 \rightarrow {}^7F_{5,6}$, which are located in the infrared region ($\approx$11 300 cm^{-1} and $\approx$10 500 cm^{-1}). The emitting ^5D_J multiplets can be efficiently populated by exciting Sm^{2+} ions into the $4f^55d^1$ configuration by the intense parity-allowed $4f^6 \rightarrow 4f^55d^1$ transitions in the spectral region above $\approx$19 000 cm^{-1}. Strong dependences on temperature and pressure were observed for the relative intensities among the $^5D_{0-2}$ multiplets which are ascribed to an influence of the $4f^55d^1$ configuration.

All the observed fluorescence lines were assigned to one single center with C_{4v} site symmetry. In the next sections, these assignments are separately discussed for Sm^{2+}:BaFCl and Sm^{2+}:SrFCl.

A. Sm^{2+}:BaFCl

A CF analysis for Sm^{2+} in BaFCl at ambient pressure has been performed by Gâcon *et al.*[20] Starting from these results, an attempt was made to assign all the observed fluorescence spectra. The pressure-induced line shifts show that (i) some fluorescence lines of the $^5D_2 \rightarrow {}^7F_J$ transitions had been assigned erroneously and (ii) the $^5D_2 \rightarrow {}^7F_4$ spectrum, which was not identified before, is also assigned in the present work.

Figure 5 gives the pressure-induced line shifts for the transitions $^5D_{0-2} \rightarrow {}^7F_0$ up to 8 GPa. In the $^5D_{1,2} \rightarrow {}^7F_0$ spectra, two symmetry-allowed lines were observed, respectively. Because the multiplets $J = 0$–2 in the C_{4v} site symmetry are splitted into one (A_1), two (E, A_2), and four (A_1,E,B_1,B_2) CF levels, respectively, the complete CF level schemes of $^5D_0$ and $^5D_1$ can be determined from the $^5D_{0,1} \rightarrow {}^7F_0$ transitions. Two CF levels (A_1 and E) of $^5D_2$ result from the $^5D_2 \rightarrow {}^7F_0$ spectrum. The other two CF levels (B_1 and B_2) of $^5D_2$ are deter-

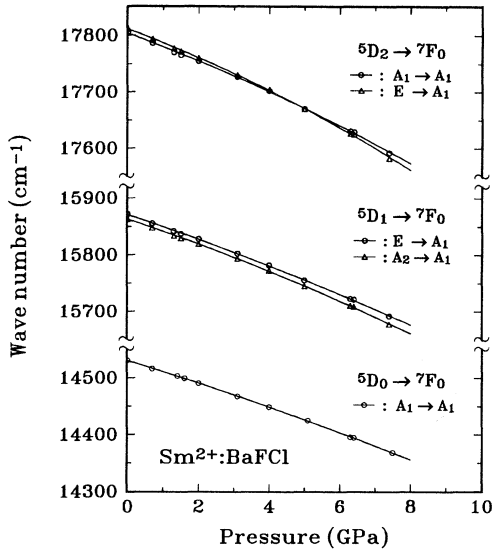

FIG. 5. Line shifts of the transitions ${}^5D_{0-2} \rightarrow {}^7F_0$ for Sm^{2+}:BaFCl under pressure.

mined from the other ${}^5D_2 \rightarrow {}^7F_J$ transitions.

For example, the ${}^5D_2 \rightarrow {}^7F_1$ transition allows to determine the CF levels of both ${}^5D_2$ and ${}^7F_1$. Figure 6 shows some typical spectra of this transition at different pressures. In principle, there are six symmetry-allowed transitions. The five lines, being electric dipole allowed, were experimentally observed, but the magnetic dipole transition ${}^5D_2(A_1) \rightarrow {}^7F_1(A_2)$ was not observed. The two CF levels within ${}^7F_1$ can be determined easily from the ${}^5D_{0,1} \rightarrow {}^7F_1$ spectra under pressure and a crossing

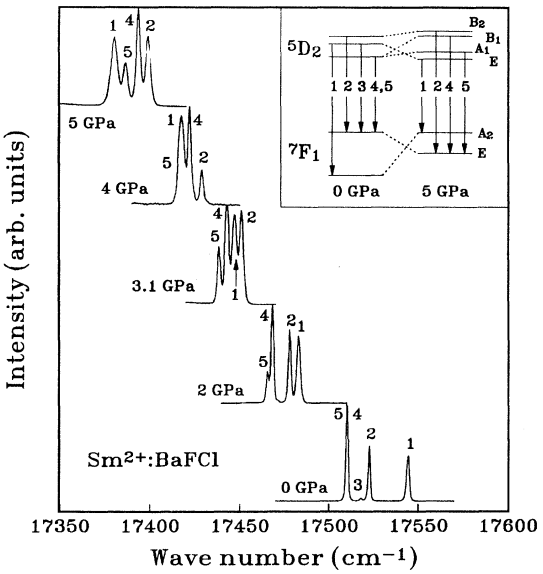

FIG. 6. Fluorescence spectra of ${}^5D_2 \rightarrow {}^7F_1$ for Sm^{2+}:BaFCl at 20 K and different pressures. The line assignments are shown with schematic level diagrams for ambient pressure and 5 GPa.

of the two CF levels of ${}^7F_1$ was observed at about 4 GPa as noted in a preliminary report.[22] From the information about ${}^7F_1$ and ${}^5D_2$ (see Fig. 5), the lines 1 and 3 can be assigned easily as shown in Fig. 6. The lines 2, 4, and 5 belong to the same final CF level ${}^7F_1(E)$. According to the above consideration, the line 2 can originate only from a transition between the initial CF level B_1 or B_2 and the final ${}^7F_1(E)$.

There is still a problem for the assignments of the lines 4 and 5, which overlap at ambient pressure and were identified as the transition ${}^5D_2(A_1) \rightarrow {}^7F_1(E)$ in the previous study.[20] These two overlapping lines are separated gradually with increasing pressure and there are two possible assignments. The first one could be based on a pressure-induced lowering of the site symmetry, which would result in the additional CF splitting of the doubly degenerate level ${}^7F_1(E)$, so that two separate lines appear under pressure. This possibility is certainly eliminated, because no additional CF splittings were observed for the other doubly degenerate levels E in any of the spectra. Therefore, an accidental energy degeneracy of the CF level ${}^5D_2(A_1)$ with one of the two unkown CF levels ${}^5D_2(B_1)$ and ${}^5D_2(B_2)$ must be assumed. Together with the experimental result about the line 2, which can possibly come from the initial CF level ${}^5D_2(B_2)$, the line 4 is assigned as ${}^5D_2(B_1) \rightarrow {}^7F_1(E)$. Of course, the line 5 results from ${}^5D_2(A_1) \rightarrow {}^7F_1(E)$, so that the pressure shift of the line 5 must be consistent with the pressure dependences of the CF levels ${}^5D_2(A_1)$ and ${}^7F_1(E)$. Figure 7 represents the relative CF splittings of the ${}^5D_2$ multiplet with respect to the multiplet centroid in the pressure region up to 8 GPa.

The accidental energy degeneracy of ${}^5D_2(A_1)$ and ${}^5D_2(B_1)$ is also confirmed by an experimental and theoretical study on the two-photon transition ${}^7F_0 \rightarrow {}^5D_2$ of Sm^{2+}:BaFCl.[23] Thus, the early assignment[20] of the CF level ${}^5D_2(B_1)$ must be rejected. In the ${}^5D_2 \rightarrow {}^7F_J$ spectra concerning the initial CF levels ${}^5D_2(A_1)$ and ${}^5D_2(B_1)$, most of the line assignments in the earlier work must be corrected due to this initial energy degeneracy

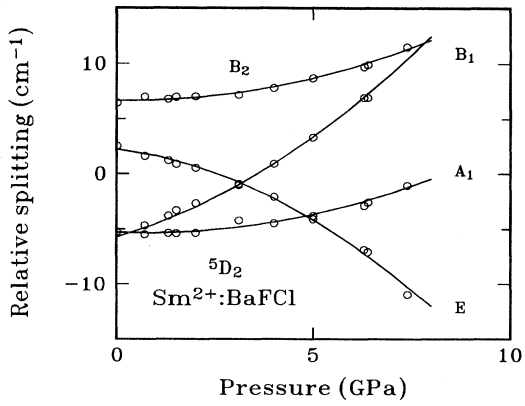

FIG. 7. CF splittings of ${}^5D_2$ for Sm^{2+}:BaFCl with respect to the multiplet centroid under pressure. The multiplet centroid of ${}^5D_2$ is located at 17 814(2) cm^{-1} at 20 K and ambient pressure and shifts with the rate of 29(2) cm^{-1}/GPa under pressure.

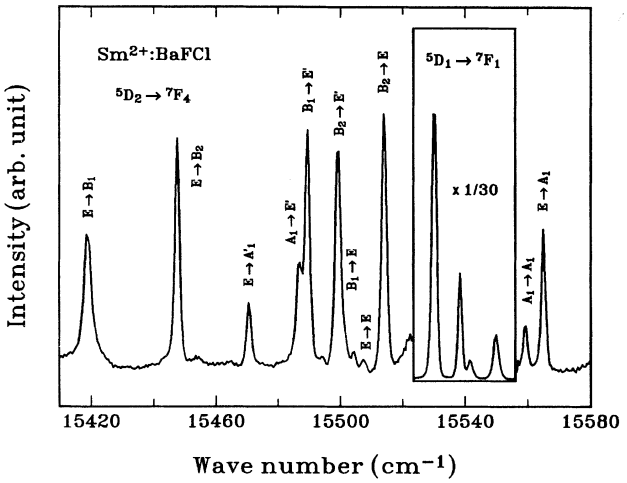

FIG. 8. Fluorescence spectra of $^5D_2 \rightarrow {}^7F_4$ for Sm^{2+}:BaFCl at 20 K and 2 GPa.

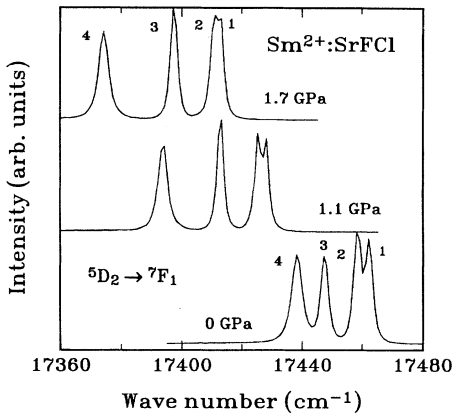

FIG. 9. Typical fluorescence spectra of $^5D_2 \rightarrow {}^7F_1$ for Sm^{2+}:SrFCl at 20 K and different pressures.

of the two levels.

By means of the pressure-induced line shifts of the transitions $^5D_{0-2} \rightarrow {}^7F_4$, the $^5D_2 \rightarrow {}^7F_4$ spectra for Sm^{2+}:BaFCl are completely identified for the first time in the present work. Figure 8 shows a typical spectrum of $^5D_2 \rightarrow {}^7F_4$ at 2 GPa and 20 K with the corresponding assignments.

B. Sm^{2+}:SrFCl

The fluorescence spectra of Sm^{2+}:SrFCl turn out to be very similar to those of Sm^{2+}:BaFCl. All the spectral features are observed at 20 K and up to 8 GPa, only the $^5D_2 \rightarrow {}^7F_J$ spectra are no longer discernible at pressure above 4 GPa.

The line assignments of the spectra for Sm^{2+}:SrFCl proceeded in the same way as for Sm^{2+}:BaFCl. In the present case, an accidental degeneracy of two other CF levels $^5D_2(B_1)$ and $^5D_2(E)$ was found at ambient pressure and removed by pressure. This fact is clearly illustrated by the $^5D_2 \rightarrow {}^7F_1$ spectra at different pressures, as shown in Fig. 9. A previous study[21] assigned the transitions $^5D_2(B_2) \rightarrow {}^7F_1(E)$, $^5D_2(E) \rightarrow {}^7F_1(E)$, $^5D_2(A_1) \rightarrow {}^7F_1(E)$, and $^5D_2(E) \rightarrow {}^7F_1(A_2)$ to the fluorescence lines 1–4 of Fig. 9, however, the pressure dependent shifts are only consistent with an assignment of $^5D_2(B_1) \rightarrow {}^7F_1(E)$ to the fluorescence line 2, whereas the other assignments are confirmed as illustrated in Fig. 10, which shows the effect of pressure on the four CF levels of $^5D_2$. Thereby, the continuous and broken lines numbered 1, 4, 3, and 2 represent values, which are calculated from the $^5D_2 \rightarrow {}^7F_1$ transition with the use of $^7F_1$ levels from $^5D_{0,1} \rightarrow {}^7F_1$ transitions, whereas the open and closed circles represent the direct results of $^5D_2(E) \rightarrow {}^7F_0$ and $^5D_2(A_1) \rightarrow {}^7F_0$ transitions, respectively. Due to the different shifts, the line 2 of Fig. 9 can be assigned thereby only to the $^5D_2(B_1) \rightarrow {}^7F_1(E)$ transition.

Furthermore, the previous determination of the CF levels for $^7F_6$ was based only on the $^5D_2 \rightarrow {}^7F_6$ transition, whereas the present study includes also the $^5D_1 \rightarrow {}^7F_6$ spectrum as shown in Fig. 11 for ambient pressure and 20 K. With the three additional CF levels $^7F_6(B_1)$, $^7F_6(B_1')$, and $^7F_6(B_2)$, not obtained in the previous study, all the CF levels of $^7F_6$ are unambiguously determined now from the present spectra.

C. Summary of CF level shifts

A complete summary and comparison of the CF level shifts for Sm^{2+}:BaFCl and Sm^{2+}:SrFCl according to the assignments of Secs. IV A and IV B is finally presented in Figs. 12 and 13.

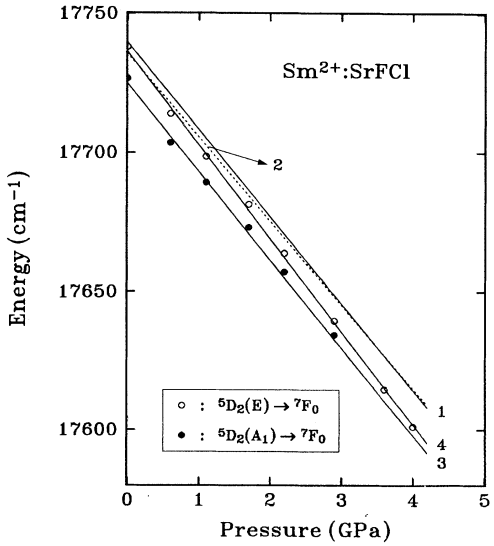

FIG. 10. Energy level shifts of $^5D_2$ for Sm^{2+}:SrFCl under pressure. Open and close circles correspond to the results directly taken from the $^5D_2 \rightarrow {}^7F_0$ spectra under pressure. The lines 1–4 correspond to the CF level positions of $^5D_2$, which are calculated by adding the four fluorescence line positions of $^5D_2 \rightarrow {}^7F_1$ to the two CF levels of $^7F_1$ determined from the $^5D_{0-1} \rightarrow {}^7F_1$ spectra.

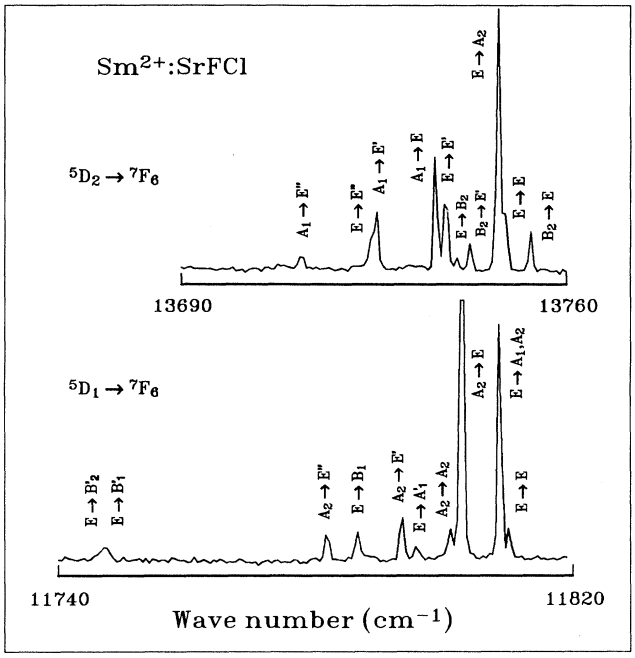

FIG. 11. The $^5D_{1,2} \rightarrow {}^7F_6$ spectra of Sm^{2+}:SrFCl at 20 K and ambient pressure.

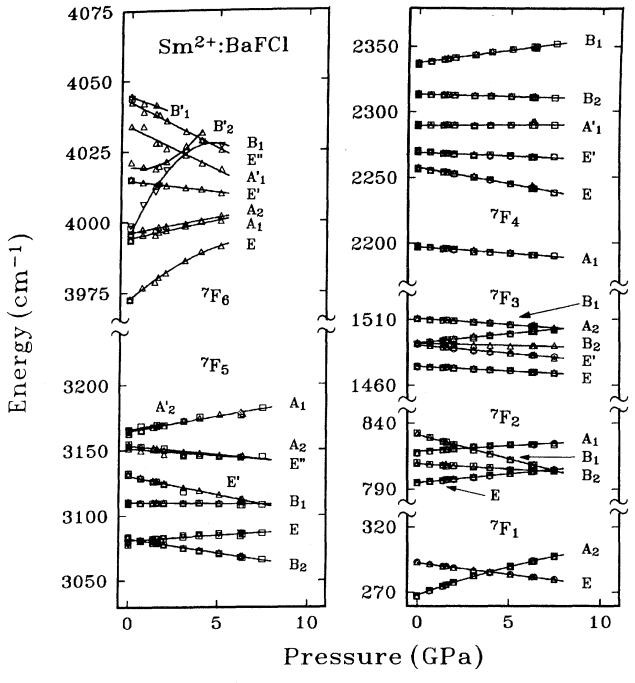

FIG. 12. Effect of pressure on the CF levels of ^7F_J for Sm^{2+}:BaFCl. Triangles, squares, and circles denote the results from the $^5D_2 \rightarrow {}^7F_J$, $^5D_1 \rightarrow {}^7F_J$, and $^5D_0 \rightarrow {}^7F_J$ transitions, respectively.

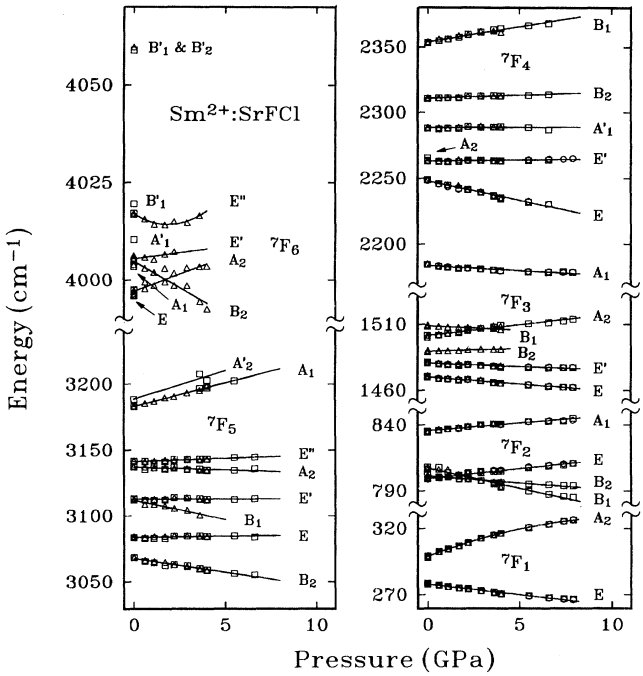

FIG. 13. Effect of pressure on the CF levels of ^7F_J for Sm^{2+}:SrFCl. Triangles, squares, and circles denote the results from the $^5D_2 \rightarrow {}^7F_J$, $^5D_1 \rightarrow {}^7F_J$, and $^5D_0 \rightarrow {}^7F_J$ transitions, respectively.

V. CRYSTAL FIELD PARAMETERS AND SUPERPOSITION MODEL

A. Crystal field parameters

The crystal field Hamiltonian $\mathcal{H}_{CF}$ in the one-electron approximation[24] can be expressed for the C_{4v} site symmetry of Sm^{2+} ions in MFX-type hosts as follows:

$$\mathcal{H}_{CF}(C_{4v}) = B_0^2 C_0^2 + B_0^4 C_0^4 + B_4^4 (C_4^4 + C_{-4}^4) + B_0^6 C_0^6 + B_4^6 (C_4^6 + C_{-4}^6) ,$$

where C_q^k are tensor operators. The splittings induced by this crystal field are calculated with the aid of eigenvalue procedures for $\mathcal{H}_{CF}$. The matrix elements of the tensor operators C_q^k can be calculated exactly, because they depend only on electronic angular coordinates. B_q^k are purely phenomenological CF parameters, which are usually obtained by least-squares fitting procedures.

The $4f^6$ configurations of Sm^{2+} or Eu^{3+} can split in C_{4v} site-symmetry into 398 A_1, 363 A_2, 379 B_1, 379 B_2, and 742 E CF levels. The corresponding energy matrix of $\mathcal{H}_{CF}(C_{4v})$ would be too large to completely deal with this configuration, however, it is possible to evaluate CF parameters within the ^7F_J multiplets, because these multiplets are relatively isolated from the other multiplets ^5D_J, ^5L_J, ^5G_J, ... of the $4f^6$ configuration.

A direct study on the truncation effect for Eu^{3+} in 15 different host crystals shows[25] that all ^7F_J crystal field splittings are practically identical in the different basis

sets. This fact indicates that the CF interaction does not lead to a significant admixture from the other multiplets to ^7F_J. Thus, it is reasonable to restrict $\mathcal{H}_{CF}(C_{4v})$ to the subspace spanned by the 49 basis vectors of ^7F_J. The 49×49 energy matrix can then be broken up further into the direct sum of six submatrices 7 A_1, 6 A_2, 6 B_1, 6 B_2 and two times 12 E.

With these considerations in mind, the CF parameters B_q^k for Sm^{2+}:BaFCl and Sm^{2+}:SrFCl were evaluated with and without J mixing. The results for B_q^k at ambient pressure are listed in Table I which shows no significant difference with and without J mixing. These data agree also perfectly with earlier results.[20,21] The variation of the CF parameters B_q^k with pressure was determined by least squares fitting to the experimentally determined CF levels (see Figs. 12 and 13) as shown in Fig. 14 by the continuous lines. One may notice as common characteristics in the variations of the CF parameters up to 8 GPa: (i) Both B_0^4 and B_0^6 increase with pressure with total changes of 15% for B_0^4 and 32% for B_0^6; (ii) B_4^6 decreases with pressure with a change of 12% for Sm^{2+}:BaFCl and 8% for Sm^{2+}:SrFCl; (iii) B_0^2 increases strongly with pressure and changes its sign at about 4 GPa in the case of Sm^{2+}:BaFCl; and (iv) B_4^4 increases with a rate of about 10 cm^{-1} GPa^{-1} with a change of sign in the case of Sm^{2+}:SrFCl.

B. Superposition model

According to the superposition model (SM),[26] the crystal field can be expressed as a sum of contributions from the individual ligands. In particular, each crystal field parameter can be written as

$$B_q^k = \sum_L \overline{B}_k(R_L) K_{kq}(\Theta_L, \Phi_L), \tag{1}$$

where the sum is over the ligands at (R_L, Θ_L, Φ_L) and the coordination factors $K_{kq}(\Theta_L, \Phi_L)$ are only functions of the ligand angular directions. $\overline{B}_k(R_L)$ are called intrinsic CF parameters for the ligand L at the distance R_L from the central $4f$ ion. This model allows (i) to separate the phenomenological CF parameters B_q^k into the geometric and the distance-dependent parts and (ii) to reduce the number of CF parameters B_q^k to three intrinsic CF parameters $\overline{B}_2$, $\overline{B}_4$, and $\overline{B}_6$.

In the SM frame, all the contributions from the ligands are absorbed into the intrinsic CF parameters. These parameters should depend only upon the ligand type and on the interionic distance. The distance dependence of the intrinsic CF parameters is usually written as a power-law expression:

$$\overline{B}_k(R) = \overline{B}_k(R_0) \left(\frac{R_0}{R} \right)^{t_k}, \tag{2}$$

where R_0 is arbitrarily chosen as a reference distance. In this sense, possible systematics for $\overline{B}_k(R_0)$ and t_k should allow to make reasonable predictions on the CF parameters for a given $4f$ ion in different host systems with the same ligand.

In the present study, the SM is also expected to be applicable to both Sm^{2+}:BaFCl and Sm^{2+}:SrFCl. When the contributions from surrounding ligands of Sm^{2+} in MFCl are taken into account (see Fig. 1), B_0^k and B_4^k (k = 4 and 6) can be expressed by the use of Eqs. (1) and (2) as follows:

$$\begin{aligned} B_0^k &= \overline{B}_k(R_{Cl}) \overline{K}_{k0}^{Cl} + \overline{B}_k(R_F) K_{k0}^F, \\ B_4^k &= \overline{B}_k(R_{Cl}) K_{k4}^{Cl} + \overline{B}_k(R_F) K_{k4}^F, \end{aligned} \tag{3}$$

where

$$\overline{K}_{k0}^{Cl} = K_{k0}^{Cl} + \left(\frac{R_{Cl}}{R_{Cl'}} \right)^{t_k^{Cl}}.$$

In Eq. (3) K_{kq}^{Cl} and K_{kq}^F are defined as collective coordination factors for 4 Cl^- and 4 F^- ligands at equidistant sets R_{Cl} and R_F, respectively, and are calculated at each pressure from the given values of Θ_{Cl} and Θ_F. To determine $\overline{B}_k(R_{Cl})$ and $\overline{B}_k(R_F)$ from the CF parameters B_0^k and B_4^k (Fig. 14) by the use of the two linear equations (3) at each pressure, one has to start with an initial value for the exponent t_k^{Cl}, because $\overline{K}_{k0}^{Cl}$ depends on this exponent. An iteration leads finally to self-consistent values. Figure 15(a) represents the final results on $\overline{B}_4(R)$ and $\overline{B}_6(R)$ for the ion pairs Sm^{2+}-F^- and Sm^{2+}-Cl^- up to 8 GPa.

TABLE I. Crystal field parameters B_q^k (cm^{-1}) at ambient pressure. N is the number of levels used in the fits and σ denotes the standard deviation between measured and calculated energy levels.

	Sm^{2+}:BaFCl		Sm^{2+}:SrFCl	
	with J mixing	without J mixing	with J mixing	without J mixing
B_0^2	−93(2)	−96(2)	63(2)	60(2)
B_0^4	−173(4)	−174(6)	−220(4)	−220(4)
B_4^4	−83(3)	−82(5)	−17(4)	−20(4)
B_0^6	398(5)	401(7)	492(5)	482(5)
B_4^6	−194(3)	−196(4)	−231(3)	−236(3)
N	35		37	
σ	1.4	2.0	1.5	1.6

At a first glance the two data sets for Sm^{2+}:BaFCl and Sm^{2+}:SrFCl in Fig. 15(a) seem to exhibit quite different power-law dependences not only for Sm^{2+}-F^- with respect to Sm^{2+}-Cl^- but also for the two different host crystals, in contrast to what one expects from the SM. However, this apparent failure of the SM can be traced back to local distortions around the $4f$ ions in the doped crystals. For Sm^{2+} in SrFCl one can safely neglect the local distortions, since the ionic radii of Sm^{2+} and Sr^{2+} are almost identical and the structural parameters for SmFCl and SrFCl at ambient conditions as well as under pressure also are very similar.

However, for Sm^{2+} in BaFCl one has to take into account local distortions, because the ionic radius for Sm^{2+} is much smaller than for Ba^{2+}. Thus, one can expect that the ligands around the Sm^{2+} ion in this host are distorted from the equilibrium host crystal positions. With

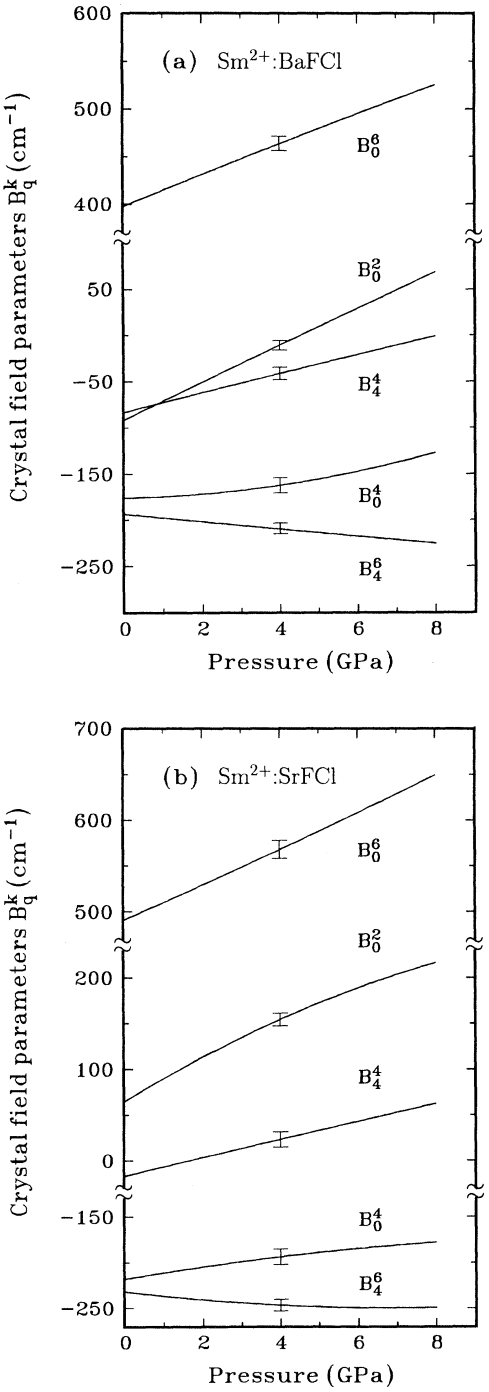

FIG. 14. Variation of CF parameters of (a) Sm^{2+}:BaFCl and (b) Sm^{2+}:SrFCl under pressure. Error bars represent the statistical errors only.

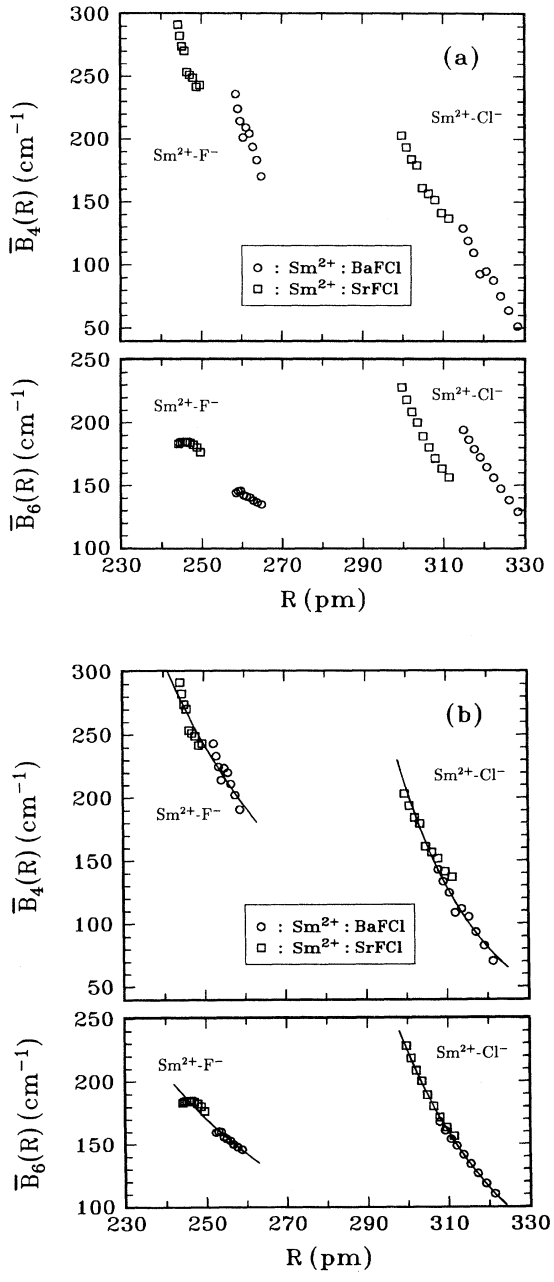

FIG. 15. Distance dependence of intrinsic CF parameters $\overline{B}_4(R)$ and $\overline{B}_6(R)$ for Sm^{2+}-Cl^- and Sm^{2+}-F^-. (a) Without and (b) with the local distortions taken into account for the case of Sm^{2+}:BaFCl (see text).

TABLE II. Intrinsic CF parameters $\overline{B}_k(R^0)$ (cm^{-1}) and the power-law exponents t_k for Sm^{2+} in BaFCl and SrFCl. The values for the reference distances R^0 (pm) correspond to SrFCl at ambient pressure.

	$\overline{B}_4(R^0)$	t_4	$\overline{B}_6(R^0)$	t_6
$Sm^{2+} - Cl^-$	124(14)	14(4)	152(16)	10(3)
$Sm^{2+} - F^-$	245(25)	5.8(1.5)	172(18)	4.6(1.1)

an adjustment of the distances R_{Cl} and R_F alone, one does not yet resolve the problem, but also minor changes in Θ_{Cl} and Θ_F have to be taken into account. Self-consistent power-laws are finally obtained with the following values for the local distortions around Sm^{2+} in BaFCl: $\Delta R_{Cl} = -7$ pm, $\Delta R_F = -6$ pm, $\Delta\Theta_{Cl} = -1°$, and $\Delta\Theta_F = -1°$. The corresponding results in Fig. 15(b) illustrate that the two data sets of Sm^{2+} in BaFCl and SrFCl fall now one common curve as expected in the SM. The respective values for $\overline{B}_k(R^0)$ and t_k are given in Table II, where the reference distances $R^0_{Cl} = 311.4$ pm and $R^0_F = 249.6$ pm correspond to the values for SrFCl at ambient condition.

The negative values for $\Delta\Theta_{Cl}$ and $\Delta\Theta_F$ reflect a displacement of the Sm^{2+} ion in BaFCl towards the plane of the neighboring F ions. This conclusion is directly supported by EPR studies on Mn^{2+} and Eu^{2+} in SrFCl,[29] where much larger displacements of 30 to 60 pm were estimated for these different ions.

To compare the present results with those of the other trivalent and divalent ions in different hosts with Cl^- or F^- ligands, other results of SM analyses are also included in Table III. Thereby, the intrinsic CF parameters for Sm^{2+}:SrF_2 and Tm^{2+}:MF_2 (M = Ba, Sr, and Ca) were derived from the literature data for the CF levels. In the cubic structure of fluorides, MF_2, there are only two CF parameters, B^4_0 and B^6_0, from which the intrinsic CF parameters $\overline{B}_k$ are directly obtained by the relations:

$$B^4_0 = -\frac{28}{9}\overline{B}_4 \quad \text{and} \quad B^6_0 = \frac{16}{9}\overline{B}_6.$$

In the case of Tm^{2+}:MF_2 the CF parameters B^4_0 and B^6_0 were evaluated from the literature data,[30] taking into account J mixing. The intrinsic CF parameters are then determined from the above given forms. Since Yeung[31] derived also the local distortions around substitutional Tm^{2+} ions on cubic sites in fluorides, these data were taken into account in the evaluation of the intrinsic CF parameters $\overline{B}_k$ at $R^0 = 251.1$ pm and for the power-law exponents t_k, which are then also given in Table III.

In the same way, the CF parameters of Sm^{2+}:SrF_2 are fitted to the CF splittings of ^7F_J multiplets observed by Wood and Kaiser.[32] In the fitting procedure, four precisely assigned CF levels (two from $^7F_2$ and two from $^7F_5$) are used at first to evaluate the parameters B^4_0 and B^6_0. Then, using these two parameters the three CF levels for $^7F_3$ are calculated with the energy sequence $^1\Gamma_2 > {}^3\Gamma_5 > {}^3\Gamma_4$ and it is noticed that the strong line at 13 140 cm^{-1}, which was assigned to $^1\Gamma_1(^5D_0) \rightarrow {}^3\Gamma_4(^7F_3)$ by Wood and Kaiser, should correspond to $^1\Gamma_1(^5D_0) \rightarrow {}^3\Gamma_5(^7F_3)$. The present assignment for this line is not in contradiction with the Zeeman splittings observed by Wood and Kaiser, because the level $^3\Gamma_5(^7F_3)$ has the same threefold degeneracy as $^3\Gamma_4(^7F_3)$. When the final fitting includes the $^7F_3$ levels, B^4_0 is not affected, but B^6_0 shows a 12% uncertainty. The resulting intrinsic CF parameters are also included in Table III.

In the case of Tm^{2+}:$SrCl_2$, the intrinsic CF parameters are calculated directly from the experimental CF parameters.[33] The distance between Sr^{2+} and Cl^- in $SrCl_2$ is $R = 302.1$ pm.[34] With the assumption that the relative local distortion $\Delta R/R$ for Tm^{2+} in $SrCl_2$ is approximately the same as for Tm^{2+} in SrF_2 given by Yeung,[31] one obtains for the Tm^{2+}-Cl^- distance $R = 295.4$ pm, which is very close to the reference value used in Table III.

The comparison of the intrinsic CF parameters and the power-law exponents given in Table III for various divalent and trivalent lanthanide ions in different host crystals shows the following results.

Cl^- Ligands. Whereas the intrinsic CF parameters $\overline{B}_k$ for the divalent ion Sm^{2+} show the same values as for the

TABLE III. Intrinsic CF parameters $\overline{B}_k(R^0)$ (in cm^{-1}) and power-law exponents t_k for lanthanide (L) ions and different hosts with fixed $R^0_{Cl} = 295.0$ pm and $R^0_F = 251.1$ pm and M = Ba, Sr, and Ca. The values for b and e are directly taken from Refs. 27 and 28 and for a, c, and d are derived from literature data as discussed in the text.

	$\overline{B}_4(R^0_{Cl})$	t_4^{Cl}	$\overline{B}_6(R^0_{Cl})$	t_6^{Cl}
Sm^{2+} : BaFCl Sm^{2+} : SrFCl	258(29)	14(4)	261(28)	10(3)
[a] Tm^{2+} : $SrCl_2$	190	—	≈ 97	—
[b] Pr^{3+} : LCl_3 Nd^{3+} : LCl_3	256(28)	4(4)	268(31)	6(2)
	$\overline{B}_4(R^0_F)$	t_4^F	$\overline{B}_6(R^0_F)$	t_6^F
Sm^{2+} : BaFCl Sm^{2+} : SrFCl	237(25)	5.8(1.5)	167(18)	4.6(1.1)
[c] Sm^{2+} : SrF_2	470(40)	—	393(50)	—
[d] Tm^{2+} : MF_2	329(35)	9.6(5)	164(15)	9.7(5)
[e] Pr^{3+} : LaF_3	533(15)	6.1(1.3)	388(50)	8.7(1.1)

trivalent ions Pr^{3+} and Nd^{3+}, the exponents t_k for Sm^{2+} are much larger than those for the two trivalent ions.

F^- Ligands. The intrinsic CF parameters $\overline{B}_k$ for Sm^{2+} in SrF_2 and Pr^{3+} in LaF_3 show roughly the same values, and the results for Tm^{2+} in MF_2 may indicate that the t_k values for divalent ions could be systematically larger than for trivalent ions. The observation that the intrinsic CF parameter $\overline{B}_4$ for Tm^{2+} is slightly smaller than for Sm^{2+} in the case of Cl^- ligands as well as in SrF_2 could be explained by a contracted radial wave function for Tm^{2+}, however, the values for $\overline{B}_6$ of Tm^{2+} for Cl^- and F^- ligands appear to be unusually small. Furthermore, one can see from Table III that the ratios $\overline{B}_6/\overline{B}_4 \approx 1.03$ for Sm^{2+}, Pr^{3+}, and Nd^{3+} in the case of Cl^- ligands and $\overline{B}_6/\overline{B}_4 \approx 0.76$ for Sm^{2+} and Pr^{3+} in the case of F^- ligands seem to give constant characteristic values.

The decrease in the ionic radii for the lanthanide (L) series with increasing atomic number leads at first to the suspicion that the intrinsic CF parameters may exhibit a similar decrease, however, the experimental data do not reflect this expectation. In particular, one can notice that $\overline{B}_6/\overline{B}_4$ changes for L^{3+} in $LaCl_3$ from a common value of about 0.91 in the first half of the lanthanide series down to a value around 0.61 in the second part. This sudden decrease has been attributed to effects from the spin-correlated crystal field, whose contributions change sign at the half-filling of the $4f$ shell (see Ref. 26). In the case of L^{3+} in LaF_3 the same effect is found with $\overline{B}_6/\overline{B}_4 \approx 0.73$ for Pr^{3+} in comparison with $\overline{B}_6/\overline{B}_4 \approx 0.53$ for Er^{3+} (see Ref. 35). Thus, the small values for the intrinsic CF parameter $\overline{B}_6$ of Tm^{2+} can be attributed to this effect.

On the other hand, the values of $\overline{B}_k(R_F^0)$ and t_k^F for the F^- ligands are unreasonably small for Sm^{2+} in BaFCl and SrFCl, which could indicate some limitations of the SM, due to ligand-ligand interactions which are not included in the SM. The effects have not been investigated systematically for the present system but, on the basis of some investigations for $PrCl_3$ which included ligand-ligand overlap effects,[36] one can expect contributions to the intrinsic CF parameters of the order of 10%. It would not be surprising if these interactions show up most strongly in those host systems, where two sets or two kinds of ligands contribute to the the CF parameters of the lanthanide ions. In the case of Er^{3+}:YAG[26], one finds some indications that this effect leads to an unreasonably small power-law exponent $t_6 = 2.3$ due to two inequivalent O^{2-} ligands which give opposite contributions (positive and negative) to the CF parameters B_2^6 and B_6^6.

In the case of Sm^{2+}:SrFCl at ambient pressure, the collective coordination factors in Eq. (3) show also partial cancellation: $K_{44}^{Cl} = 1.616$, $K_{44}^{F} = -0.978$, $K_{64}^{Cl} = 0.360$, and $K_{64}^{F} = -1.625$. Due to the opposite signs of the factor pairs $(K_{44}^{Cl}, K_{44}^{F})$ and $(K_{64}^{Cl}, K_{64}^{F})$, there can be a strong cancellation between the contributions coming from the Cl^- and from F^- ligands, which results in the small values for $\overline{B}_4(R_F^0)$ and $\overline{B}_6(R_F^0)$. If the contributions of the ligand-ligand interactions could be separated from the experimental values of B_q^k, one might obtain larger values of $\overline{B}_k$ for F^- ligands and smaller values for Cl^- ligands, which would explain the anomalies for Sm^{2+} in the MFCl hosts.

Under pressure, the ligand-ligand interactions are becoming stronger and induce thereby also larger corrections in the evaluation of intrinsic CF parameters. This would mean that the exponents t_k^F become larger and the exponents t_k^{Cl} smaller, which could explain also the difference with respect to Tm^{2+}.

In summary, in both cases of F^- and Cl^- ligands, (i) the intrinsic CF parameters $\overline{B}_4$ and $\overline{B}_6$ for trivalent and divalent ions with less than the half-filled $4f$ shells are very similar, and (ii) the power-law exponents t_k for divalent ions appear to be systematically larger than for trivalent ions. In the comparison of F^- with Cl^- ligands, the $\overline{B}_k$ values for F^- appear to be always larger than for Cl^-.

VI. CONCLUSIONS

The present investigation of the CF levels for Sm^{2+} in the host crystals BaFCl and SrFCl under pressure results, in the framework of the SM, not only in the intrinsic CF parameters $\overline{B}_k$ and but also in their distance dependences t_k for Sm^{2+} with Cl^- and F^- ligands.

The comparison with results for trivalent lanthanide ions shows for Cl^- and F^- ligands larger power-law exponents t_k for the divalent lanthanide ions, whereas the intrinsic CF parameters for both divalent and trivalent lanthanide ions are very similar in magnitude, however, with larger values for the $\overline{B}_k$ of F^- in comparison with Cl^- ligands as expected within the SM.

In the present case of Sm^{2+} in MFCl with two different kinds of ligands, the SM gives self-consistent results only when ligand-ligand interactions are taken into account for the F^- ligands.

Finally, it can be noted that other isostructural compounds like CaFCl, MFBr, and MFI for divalent ions or LOX for trivalent ions offer interesting hosts for systematical studies in ever wider pressure ranges and some of these studies are presently in progress.

ACKNOWLEDGMENTS

We are indebted to D. Niggemeier for sample preparation and to T. Hangleiter for his help in the absorption measurements.

[1] R. Jaaniso and H. Bill, Europhys. Lett. **16**, 569 (1991).
[2] Y. R. Shen, T. Gregorian, and W. B. Holzapfel, High Press. Res. **7**, 73 (1991).
[3] B. Lorenz, Y. R. Shen, and W. B. Holzapfel, High Press. Res. **12**, 91(1994).
[4] W. von der Ahe, Diploma thesis, Universität Paderborn, 1989.
[5] G. J. Piermarini, S. Block, J. D. Barnet, and R. A. Forman,

J. Appl. Phys. **46**, 2774 (1975).
[6] R. A. Noack and W. B. Holzapfel, in *High Pressure Science and Technology*, edited by K. D. Timmerhaus and M. S. Barber (Plenum, New York, 1979), Vol. 1, p. 748.
[7] Y. R. Shen, U. Englisch, L. Chudinovskikh, F. Porsch, R. Haberkorn, H. P. Beck, and W. B. Holzapfel, J. Phys. Condens. Matter **6**, 3197 (1994); Y. Shen, Ph.D. thesis, Universität Paderborn, 1994.
[8] H. P. Beck, A. Limmer, W. Denner, and H. Schulz, Acta Crystallogr. B **39**, 401 (1983).
[9] R. Haberkorn, Ph.D. thesis, Universität Erlangen-Nürburg, 1988.
[10] H. Bärnighausen, G. Brauer, and N. Schulte, Z. Anorg. All. Chem. **338**, 250 (1965).
[11] J. Flahaut, J. Solid. State Chem. **9**, 124 (1974).
[12] H. P. Beck, Z. Anorg. All. Chem. **451**, 73 (1979).
[13] H. P. Beck and A. Limmer, Z. Anorg. All. Chem. **502**, 185 (1983).
[14] R. D. Shanon, Acta Crystallogr. Sect. A **32**, 751 (1976).
[15] R. Narayan, Pramāna **13**, 559 (1979).
[16] M. Sauvage, Acta Crystallogr. B **30**, 2786 (1974).
[17] T. Hangleiter, F. K. Koschnick, J.-M. Spaeth, R. D. H. Nuttall, and R. S. Eachus, J. Phys. Condens. Matter **2**, 6837 (1990).
[18] Z. Kiss and H. A. Weakliem, Phys. Rev. Lett. **15**, 457 (1965).
[19] A. Dupont, J. Opt. Soc. Am. **57**, 867 (1967).
[20] J. C. Gâcon, G. Grenet, J. C. Souillat, and M. Kibler, J. Chem. Phys. **69**, 868 (1978).
[21] G. Grenet, M. Kibler, A. Gros, J. C. Souillat, and J. C. Gâcon, Phys. Rev. B **22**, 5052 (1980).
[22] Y. R. Shen and W. B. Holzapfel, J. Alloys Compounds **192**, 53 (1993).
[23] J. C. Gâcon, J. F. Marcerou, M. Bouazaoui, and B. Jacquier, Phys. Rev. B **40**, 2070 (1989).
[24] B. G. Wybourne, *Spectroscopic Properties of Rare Earths* (Wiley, New York, 1965).
[25] O. K. Moune, P. Caro, D. Garcia, and M. Faucher, J. Less-Common Met. **163**, 287 (1990).
[26] D. J. Newman and Betty Ng, Rep. Prog. Phys. **52**, 699 (1989).
[27] Th. Tröster, T. Gregorian, and W. B. Holzapfel, Phys. Rev. B **48**, 2960 (1993); Th. Tröster, Ph.D. thesis, Universität Paderborn, 1994.
[28] Y. Y. Yeung and M. F. Reid, J. Less-Common Met. **148**, 213 (1989).
[29] D. Zevenhuijzen, J. A. van Winsum, and H. W. den Hartog, J. Phys. C **9**, 3113 (1976).
[30] W. Hayes and P. H. Smith, J. Phys. C **4**, 840 (1971).
[31] Y. Y. Yeung, J. Phys. C **21**, L549 (1988).
[32] D. L. Wood and W. Kaiser, Phys. Rev. **126**, 2079 (1962).
[33] G. Burns, and J. D. Axe, in *Optical Properties of Ions in Crystals*, edited by H. M. Crosswhite and H. W. Moos (Interscience, City, 1967), p. 53.
[34] H. A. Weakliem and Z. J. Kiss, Phys. Rev. **157**, 277 (1967).
[35] Y. Y. Yeung and D. J. Newman, J. Chem. Phys. **82**, 3747 (1985).
[36] M. M. Curtis and D. J. Newman, J. Chem. Phys. **52**, 1340 (1970).

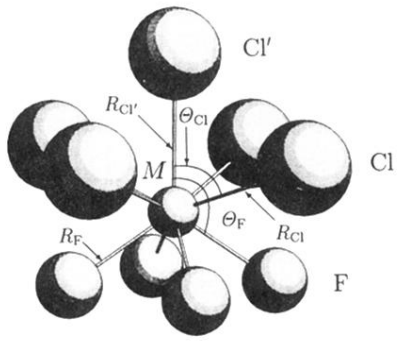

FIG. 1. Coordination polyhedron for the Cl^- and F^- ligands around the central ion M in MFCl.